Biogeosciences, 21, 5219–5231, 2024
https://doi.org/10.5194/bg-21-5219-2024

Biogeosciences Open Access EGU

Similar freezing spectra of particles in plant canopies and in the air at a high-altitude site

Annika Einbock and Franz Conen

Department of Environmental Sciences, University of Basel, 4056 Basel, Switzerland

Correspondence: Annika Einbock (annika.einbock@unibas.ch)

Received: 4 July 2024 – Discussion started: 22 July 2024
Revised: 20 September 2024 – Accepted: 24 September 2024 – Published: 25 November 2024

Abstract. Plant canopies are an important source of biological particles aerosolized into the atmosphere. Certain aerosolized microorganisms are able to freeze slightly supercooled cloud droplets and therefore affect mixed-phase cloud development. Still, spatiotemporal variability of such biological ice-nucleating particles (INPs) is currently poorly understood. Here, we study this variability between late summer and leaf shedding on the scale of individual leaves collected about fortnightly from four temperate broadleaf tree species (*Fagus sylvatica*, *Juglans regia*, *Prunus avium* and *Tilia platyphyllos*) on a hillside (Gempen, 650 m a.s.l. (metres above sea level)) and in a vertical canopy profile of one *Fagus sylvatica* (Hölstein, 550 m a.s.l.) in north-western Switzerland. The cumulative concentration of INPs active at ≥ -10 °C ($INPs_{-10}$) did not vary significantly between the investigated tree species but, as inferred from leaf mass per area and leaf carbon isotopic ratios, seemed to be lower on sun leaves as compared with shade leaves. Between August and mid-November, the median INP concentration increased from 4 to 38 $INP_{-10}\,cm^{-2}$ of leaf area and was positively correlated with mean relative humidity throughout 24 h prior to sampling (Spearman's $r = 0.52$, $p < 0.0001$, $n = 64$). In 53 of the total 64 samples collected at the Gempen site, differential INP spectra between -3 and -10 °C exhibited clearly discriminable patterns: in 53 % of the spectra, the number of additionally activated INPs increased persistently with each 1 °C decrease in temperature; the remaining spectra displayed significant peaks in differential INP concentration above -9 °C, most frequently in the temperature interval between -8 and -9 °C (21 %) and between -7 and -8 °C (17 %). Interestingly, the three most frequent patterns in differential INP spectra on leaves in Gempen were also prevalent in similar fractions in air samples with clearly discriminable patterns at the high-altitude Jungfraujoch site (3580 m a.s.l., Switzerland) collected during summer in the previous year. These findings corroborate the idea that a large fraction of the airborne biological INP population above the Alps during summer originates from plant surfaces. Which parameter or set of parameters could affect biological INP populations on both scales – upwind airsheds of high-altitude sites as well as individual leaves – is an intriguing question for further exploration. A first guess is that leaf wetness duration plays a role.

1 Introduction

Processes on the earth's surface and in the atmosphere are interrelated. Ice-nucleating particles (INPs) emitted from the earth's surface, for example, can initiate freezing in clouds at temperatures exceeding ~ -38 °C, where in their absence droplets remain liquid (Kanji et al., 2017; Murray et al., 2012). The impact on cloud physics critically depends on both total INP concentration and population properties such as individual freezing temperatures of the present INPs (Hawker et al., 2021). The dynamics of biological INPs at mixed-phase cloud height are poorly understood (Burrows et al., 2022; Cornwell et al., 2023). This is partly due to the large variety and heterogeneity of the involved particles as well as spatiotemporal variations in source activities and drivers thereof (Burrows et al., 2022; Cornwell et al., 2023).

Soil organic matter (Conen et al., 2011; Hill et al., 2016; O'Sullivan et al., 2014) and living vegetation (Felgitsch et al., 2018; Hiranuma et al., 2015; Lindemann et al., 1982; Lindow et al., 1978a; Pummer et al., 2012; Seifried et al., 2020) as well as decaying vegetation (Haga et al., 2014; Schnell

and Vali, 1976) are major sources of biological INPs. Ice-nucleating active (INA) microorganisms inhabiting these environments are among the most efficient INPs discovered so far and active at temperatures of $\geq -10\,^{\circ}\mathrm{C}$ (INPs_{-10}) (Huang et al., 2021). Recently, also INPs_{-10} originating from pollen have been identified (Gute and Abbatt, 2020; Kinney et al., 2024; Wieland et al., 2024). On a global scale, considering land cover (Latham et al., 2014) and leaf area (Vorholt, 2012), plant surfaces provide a giant reservoir of INPs_{-10} leaking into the atmosphere. An indication of the large contribution of INA microorganisms emitted from plant canopies to the INP_{-10} population at cloud height above western Europe was revealed through heat treatment of INPs at the High Altitude Research Station Jungfraujoch (JFJ, 46°32′53″ N, 07°59′02″ E, 3580 m a.s.l. (metres above sea level)) in the Swiss Alps (Conen et al., 2022). During summer and early autumn, admixture of air from the planetary boundary layer at JFJ is enhanced (Griffiths et al., 2014) and most soils in the surrounding temperate region are covered by plants. Under these conditions, the phyllosphere – plant surfaces in contact with the atmosphere (Vorholt, 2012) – in the airshed upwind presumably contributes the majority of INPs_{-10} observed at JFJ.

Ice-nucleating active microorganisms associated with the phyllosphere include various gram-negative bacteria (Kim et al., 1987; Lindow et al., 1978b; Maki et al., 1974) and fungal species (Morris et al., 2013; Pouleur et al., 1992). The ability of gram-negative bacteria to nucleate ice is rooted in the expression of ice nucleation (IN) proteins that can aggregate into assemblies of varying sizes. The largest protein clusters make freezing close to 0 °C possible (Govindarajan and Lindow, 1988; Qiu et al., 2019). Recently, such clustering has also been discovered in cell-free INPs shed by the ice-nucleating active (INA) fungus *Fusarium acuminatum* (Schwidetzky et al., 2023) and in ice-nucleating macromolecules (INMs) released by pollen of *Betula pendula* (Wieland et al., 2024). Microbial ice-nucleating activity differs between species (Huang et al., 2021) and strains (O'Brien and Lindow, 1988; Yang et al., 2022; Yankofsky et al., 1981) and may allow for the most efficient strains to draw water vapour from the atmosphere into zones of a leaf surface that would otherwise remain dry (Einbock and Conen, 2024). In addition, variations in microbial growth and environmental conditions can substantially change freezing characteristics of microbial INA populations (Hirano and Upper, 1989; Lindow et al., 1982; Nemecek-Marshall et al., 1993; O'Brien and Lindow, 1988; Richard et al., 1996; Ruggles et al., 1993; Yang et al., 2022). These variations in the expression of ice-nucleating activity and the number of known and perhaps unknown INA species, together with uncertainties concerning their cultivability, make it challenging to predict atmospheric INP dynamics from the assessment of microbial community compositions on leaf surfaces. A complementary approach to understanding the link between INPs in the phyllosphere and atmosphere is to compare differential INP spectra in both spheres. Here, we investigate INP spectra on leaves of four deciduous tree species from late summer throughout leaf senescence. We discuss trends in cumulative INP_{-10} concentrations and patterns in differential INP spectra. Finally, we compare differential INP spectra on foliage with observations of INP spectra during summer 2022 in the air at JFJ.

2 Methods

2.1 Foliage sampling

We sampled leaves of four broadleaf tree species commonly found in temperate forests near Gempen (GEP, 47°28′53″ N, 7°39′30″ E, ∼ 650 m a.s.l.) and Hölstein (HOL, 47°26′17″ N, 7°46′37″ E, ∼ 550 m a.s.l.), Switzerland. Both sampling locations are situated on hillsides in the northern Jura Mountains at a linear distance of about 10 km from each other. Sampling was conducted between early August and mid-November 2023. Samples from Gempen were collected approximately fortnightly on eight occasions. In Hölstein, we collected foliage twice, with 5 weeks in between (5 September and 11 October). Samples were collected between 09:30 and 11:30 local time, stored at 5 °C, and analysed for their INP concentration within 3–4 d.

In Gempen, we sampled leaves of two individuals of *Tilia platyphyllos*, *Fagus sylvatica* and *Juglans regia*, respectively, along a 1.5 km path through a small forest surrounded by agricultural land. Additionally, two individuals of *Prunus avium* were sampled around 50 m away from the forest edge in an adjacent meadow. We sampled trees that were the least overgrown by taller canopies of other species at more open parts of the path and aimed for the leaves that were the least likely to be affected by throughfall from canopies above. From 26 September onwards, roughly the onset of leaf colouration, the same trees were sampled on successive occasions. During the first three sampling occasions, various individuals of *T. platyphyllos* (TP1, TP2), *F. sylvatica* (FS2) and *J. regia* (JR2) had been sampled in the same segments of the path as from 26 September onwards. Foliage was cut from the trees about 1.5 to 2.5 m above ground using a pair of flame-sterilized scissors and directly transferred into polyethylene zip bags without further contact. Blank measurements had shown the zip bags did not contain INPs_{-10}. In Hölstein, covering the entire vertical extent of the canopy, foliage of a *F. sylvatica* individual was collected at about 10, 20 and 30 m above ground. Leaves were accessed from the Swiss Canopy Crane II (Kahmen et al., 2022) and sampled from the outermost canopy parts. At each height, a sample was taken from the south- and the north-facing side.

Meteorological data and atmospheric pollen concentrations were obtained from the nearest stations operated by the Swiss Federal Office of Meteorology and Climatology (MeteoSwiss) (Binningen, 47°32′ N, 7°35′ E, 316 m a.s.l.;

Basel, 47°34′ N, 7°35′ E, 256 m a.s.l.), 10 km NE of Gempen, and the Swiss Federal Institute for Forest, Snow and Landscape Research (Hölstein, 47°26′ N, 7°47′ E, 530 m a.s.l.) and obtained from the data portal IDAWEB (https://gate.meteoswiss.ch/idaweb, last access: 12 November 2024, login required) provided by MeteoSwiss. Due to the difference in altitude between Binningen and Gempen, the temperature was corrected assuming a temperature decrease of 0.65 K per 100 m of increase in altitude. Precipitation data at Gempen were obtained from the data portal of MeteoSwiss.

2.1.1 Leaf colour

Leaf colour was determined right after sampling by visually matching adaxial leaf sides to 1 of 2050 reference colours (NCS Index 2050) provided by the Natural Colour System (NCS). The NCS is a three-dimensional colour model based on human colour perception (Hård and Sivik, 1981) and has been used to assess vegetation colour in the past (Grose, 2014, 2016; Shen et al., 2022; Xing et al., 2019). Briefly, blue, red, yellow and green are considered elementary hues that are represented on a colour circle. Two neighbouring elementary hues are mixed in varying proportions to describe the hue of a colour of interest. In addition to a specific hue, each colour is assigned a nuance value which depends on its black-/whiteness and chromaticness (Hård and Sivik, 1981).

Colours were assessed on sampling days around noon beneath an east-facing window. All leaves comprising a sample were considered collectively, and the main leaf colour identified was the colour covering the largest leaf area per sample. Colour determination was performed by one or two independent observers. For the colour assessment which took a few minutes per sample, leaves were removed from the polyethylene zip bags and spread with their adaxial side up on top of a new polyethylene zip bag cleaned with 2-propanol. Samples of a leaf area of approximately 100 cm^2 (81.0 to 142.7 cm^2) corresponding to between 1 and 19 leaves were stored in 50 mL polypropylene tubes (Cellstar®, Greiner Bio-One, Switzerland) at 5 °C until INP analysis. Throughout the process, leaves were handled with gloves (Vasco®, Nitril light, B. Braun, Switzerland) cleaned with 2-propanol. For statistical analysis, NCS hue labels were converted to a length value as described by Xing et al. (2019). For visualization in Fig. 3 and Figs. S1 and S2 in the Supplement, NCS values were converted to a hex colour code using an online tool (https://www.w3schools.com/colors/colors_converter.asp, last access: 10 November 2024).

2.1.2 INP analysis

Ice-nucleating particle concentrations were quantified in leaf-washing water. Immediately before each freezing test, the tubes containing the leaf samples were filled up with 50 mL of 0.1 % NaCl in Milli-Q® water, sonicated for 1 min (RK 100, Bandelin, Germany) and shaken manually for another 20 s. Sonication for 1 min was a compromise informed by additional trials. When compared to different sonication times between 10 s and 6 min, 1 min was long enough to suspend the majority of INPs from the leaf surface while avoiding visible leaf damage that may promote the release of INPs from within the leaf structure. Leaves were removed and pressed between sheets of thick cellulose paper (Clairefontaine Goldline, 300 $g m^{-2}$, the Netherlands) until further processing. A total of 28.8 mL of leaf-washing water was transferred to two subsets of 72 Safe-Lock Tubes (Eppendorf, 0.5 mL, Germany), each containing 200 µL of the sample. The two subsets were cooled in parallel in two separate cold baths (Lauda RC6, Lauda-Königshofen, Germany) from −3 to −10 °C. After every 1 °C step in cooling (rate of 0.3 °C min^{-1}), the temperature was left unchanged for at least 30 s before the number of frozen droplets was determined visually by one observer for both subsets or two independent observers for one subset each. When a large fraction of droplets had frozen at −10 °C, additional 1 : 10 and 1 : 100 dilutions of the leaf-washing water were analysed. Where dilutions overlapped, we selected the data points from the dilution in which the fraction of frozen droplets was closest to 50 %. In cases where the pattern of a differential INP spectrum would have changed solely because of a switch between dilutions, this switch was implemented at the next possible temperature interval. Blanks consisting of the utilized 0.1 % NaCl Milli-Q® water did not freeze within the investigated temperature range. Differential INP concentrations were quantified according to Eq. (8) in Vali (2019), and cumulative INP concentrations were calculated as the sum of differential INP concentrations (Vali, 1971, 2019).

2.1.3 Leaf mass per area, carbon-to-nitrogen ratio and $\delta^{13}C$ values

Samples were dried collectively at 40 °C until their weight had stabilized. The leaf mass per area (LMA) was calculated as leaf dry weight divided by the leaf area as determined with the software WinDIAS 3 (version 3.3.0.39, Delta-T Devices, United Kingdom). The leaf carbon (C) and nitrogen (N) concentration and stable carbon isotope ratio ($\delta^{13}C$, relative to Vienna Peedee Belemnite (VPDB)) were analysed with an elemental analyser coupled to an isotope ratio mass spectrometer (EA-IRMS; Integra2, Sercon, Crewe, UK). For that purpose, a number of randomly selected punches (2 mm diameter) were taken from each dried sample and weighed in a tin capsule (0.72 to 1.68 mg per sample). Mass calibration for C and N quantification was performed with lab standard ethylenediaminetetraacetic acid (EDTA) (41.09 % C, 9.59 % N). For isotopic (C) size correction and calibration lab standard EDTA (41.09 % C, 9.59 % N), USGS61 (Coplen, 2019b) and USGS40 (Coplen, 2019a) were used. Carbon-to-nitrogen ratios (C : N ratios) are shown as atomic ratios. According to the analysed standard substances, the standard deviation for $\delta^{13}C$ is < 0.3 ‰.

2.2 Aerosol sampling and analysis

For a preceding study at JFJ, we collected over 23 d, between the beginning of July and mid-August 2022, a total of 133 aerosol samples (Einbock, 2023). The observatory JFJ is located at an elevation 3 km higher than the foliage sampling sites and situated about 110 km SSE of Gempen. About one-third of Switzerland is covered by temperate forest, and another third is agricultural land (Beyeler et al., 2021). Sampling at JFJ was conducted with a high-flow rate impinger (flow rate of 300 L min^{-1}, Coriolis μ, Bertin Technologies, France). Ambient aerosol particles were collected in 15 mL of ultrapure water (W4502-1L, Sigma-Aldrich) containing 0.5 % NaCl to reduce osmotically induced stress in biological cells (Stopelli et al., 2014). The majority of samples ($n = 129$) were collected throughout 30 min periods consisting of five consecutive 5 min intervals. For the remaining samples ($n = 4$), the impinger was operated during three consecutive 5 min intervals. Water lost during the impinger operation was replenished between the 5 min sampling intervals with NaCl-free ultrapure water. After the last 5 min interval, the liquid volume in the sampling cone was quantified. Samples were analysed with the automatic freezing detection apparatus LINDA (Stopelli et al., 2014) immediately after collection in 52 tubes (0.5 mL Eppendorf Safe-Lock, Germany), each containing 200 µL of impinger liquid. None of the analysed blanks of NaCl-containing and NaCl-free ultrapure water contained INPs active above −12 °C. As for the foliage samples, differential INP concentrations were calculated based on Eq. (8) in Vali (2019) and cumulative INP concentrations displayed as sum of differential INP concentrations (Vali, 1971, 2019). Sodium analysis of the impinger liquid (940 Professional IC Vario, Metrohm, Switzerland) revealed that its concentration decreased to 70 % of its initial concentration during the 25 min the impinger was operated. This decrease indicates some loss of liquid in the form of droplets; a loss of liquid in the form of water vapour only would not have removed NaCl. Therefore, we corrected INP concentrations for potential INP loss with droplets exiting the impinger during collection by multiplying uncorrected INP concentrations with a factor of $\frac{2}{1+0.7}$, assuming the loss of INPs is zero at the beginning of sampling, when there are no INPs in the liquid, and increasing linearly with time; i.e. the fraction of INPs lost with droplets is half the fraction of NaCl lost.

2.3 Statistically significant peaks in differential INP spectra

In immersion freezing experiments, it can be presumed that the number of INPs per droplet activated within each investigated temperature interval is Poisson distributed (Vali, 1971, 2019). Accordingly, the standard deviation of the number of INPs activated within each temperature step equals the square root of the number of freezing events in the assay within this temperature interval (Vali, 2019). We consider a temperature interval (ΔT) in a differential INP spectrum to constitute a significant peak if the sum of the standard deviations of the number of freezing events in ΔT and $\Delta(T+1)$ is smaller than the difference in the number of freezing events between ΔT and $\Delta(T+1)$, where $\Delta(T+1)$ is the next colder temperature interval after ΔT.

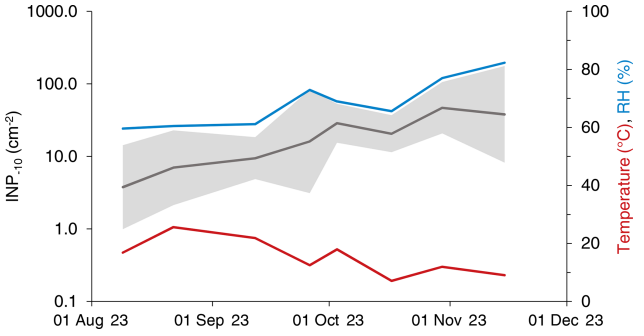

Figure 1. Temporal development of the median INP_{-10} concentration on leaves collected in Gempen (grey line), relative humidity (blue) and air temperature (red). The multiplicative standard deviation (Limpert et al., 2001) of the INP_{-10} concentration is indicated as a shaded area.

3 Results and discussion

3.1 Cumulative INP concentrations

3.1.1 Temporal trends in INP_{-10} concentrations, meteorological parameters and leaf traits

We found a total of 273 295 $INPs_{-10}$ on a leaf area (LA) of 8304 cm^2 and 733 $INPs_{-10}$ in 968 m^3 of air (local conditions). From the beginning of August until mid-November, the median INP concentration on leaves collected at GEP increased from 4 to 38 INP_{-10} cm^{-2}. The mean relative humidity (RH) throughout the 24 h prior to sampling increased from around 60 % to 82 % with a transient maximum of 73 % on September 26. The mean air temperature throughout the 24 h prior to sampling decreased from about 20 °C in August to approximately 10 °C in mid-October (Fig. 1). There was no precipitation 24 h prior to sampling during the entire campaign at both sites, except for the last sampling day in November (17.3 mm over 24 h). Cumulative INP_{-10} concentrations correlated significantly with the mean RH (Spearman's $r = 0.52$, $p < 0.0001$, $n = 64$) and mean air temperature (Spearman's $r = -0.34$, $p = 0.006$, $n = 64$), respectively. The correlation between the INP_{-10} concentration and mean RH persisted when considering the tree species separately, except for *F. sylvatica*. On the level of individual tree species, the negative correlation between the INP_{-10} concentration and mean air temperature was only significant for *P. avium*.

The activation temperature ($\geq -10\,°C$) of the investigated INPs suggests they are predominantly of biological origin (Huang et al., 2021; Kanji et al., 2017). The analysed sample type (leaf-washing water of broadleaf trees) further renders a considerable contribution of INA microorganisms to the investigated INP population likely (Hill et al., 2014; Lindow et al., 1978a). Potential additional sources of $INPs_{-10}$ at the sampling locations known at present might include INMs derived from pollen (Gute and Abbatt, 2020; Kinney et al., 2024; Wieland et al., 2024). Tree species commonly found in central European forests, including the four species investigated here, typically do not flower between August and November (Anonymous, 2002). Still, wind-dispersed pollen from other plant species and long-range transport deposited onto the leaves might have contributed to the analysed INP population. Atmospheric pollen concentrations at the Basel site are continuously monitored, and measurements for about 50 plant species or families are available until 29 September 2023, with 7 among them available until the end of the sampling period. While cumulative INP_{-10} concentrations increased on leaves, airborne pollen concentrations showed a decreasing trend. There was no correlation between pollen concentrations from individual species or families and INP_{-10} concentrations. In the following, we will therefore focus on microbial INPs.

Generally, the cumulative INP_{-10} concentration in the bacterial population on foliage is affected by both the population size and the frequency of INPs among cells (nucleation frequency, NF) (Lindow et al., 1982). The temperature (Hirano and Upper, 1989; Nemecek-Marshall et al., 1993; Ruggles et al., 1993), RH (Hirano and Upper, 1989; Leben, 1988), nutrient availability (Nemecek-Marshall et al., 1993; Ruggles et al., 1993) and plant genotype (Lindow et al., 1978a; O'Brien and Lindow, 1988), among other factors, have been found to influence the population size and NF of epiphytic bacteria, sometimes in an opposing manner. The culture age and variations in growing conditions were further found to influence the ice-nucleating activity of different *Fusarium* species (Richard et al., 1996; Yang et al., 2022).

In this study, decreasing air temperatures between late summer and autumn might have triggered an enhanced expression of IN proteins in microbes (Anderson et al., 1982; Hirano and Upper, 1989; Nemecek-Marshall et al., 1993), possibly contributing to the observed increase in INP_{-10} concentrations. The significant correlation between the air temperature and INP_{-10} concentration in *P. avium* and the absence of such a correlation in the other species might have been related to the free-standing position of *P. avium* in a meadow, while the other trees investigated were situated within a forest. Thus, the *P. avium* individuals were less shielded by surrounding trees against radiative cooling during clear nights and might have experienced lower leaf temperatures at night, pronouncing the effect of temperature on the observed INP_{-10} concentrations. Jordan and Smith (1994) found leaf temperatures during clear nights were around 4 °C below the air temperature.

Moisture promotes the survival and growth of epiphytic microorganisms (Beattie and Lindow, 1995; Grinberg et al., 2019), affects their spatial distribution within the leaf microhabitat (Doan et al., 2020), and possibly influences the composition of the phyllosphere microbiome (Beattie, 2011). Intense rain events were found to trigger an increase in the population size of the bacterial INA strain *Pseudomonas syringae* pv. *syringae* on snap bean leaflets (Hirano et al., 1996). Further, high RH fosters the abundance of *Pseudomonas syringae* in the phyllosphere (Leben, 1988) and seems to enhance ice-nucleating activity on foliage (Hirano and Upper, 1989). The strong correlation between RH and the INP_{-10} concentration observed here indicates an effect of RH on either the abundance of INA microorganisms on foliage, their NF or both, even though relationships cannot fully be disentangled due to the co-occurrence of continuous trends in INP_{-10} concentrations and meteorological parameters. An increased supply of INPs in the phyllosphere at an elevated RH might, disregarding differences in emission mechanisms, contribute to the enhanced concentration of airborne INPs observed under humid conditions (Testa et al., 2021; Wright et al., 2014).

At the seasonal scale, not only changes in climate but also leaf characteristics and plant defence during senescence have been associated with shifts in phyllosphere microbial communities in various ecosystems (Kinkel, 1997; Šigutová et al., 2023; Stone and Jackson, 2021). During senescence, leaf processes change and the nutrient content in foliage decreases considerably (Lim et al., 2007). Here, leaf colouration was mirrored in a distinct shift to larger C : N ratios and a smaller amount of N per leaf dry weight in all sampled trees (Fig. S1). Significant correlations between the INP_{-10} concentration and leaf colour NCS code expressed as the length value (Sect. 2.1.1) (Spearman's $r = 0.29$, $p = 0.02$, $n = 64$), C : N ratio (Spearman's $r = 0.39$, $p = 0.002$, $n = 64$) and amount of N per leaf dry weight (Spearman's $r = -0.41$, $p = 0.0008$, $n = 64$) were found for the entire GEP data set but were absent when green and coloured leaves were assessed separately ($p > 0.05$, $n = 38$ and $n = 26$, respectively).

3.1.2 Differences within and between trees

Cumulative INP_{-10} concentrations did not vary significantly between the investigated tree species. Rather, concentrations differed between some individual trees, e.g. between the two *F. sylvatica* individuals and the two *T. platyphyllos* individuals sampled at GEP (Fig. S2).

In the vertically sampled *F. sylvatica* (HOL), INP_{-10} concentrations increased from the top to the lowest part of the canopy. The four samples from the top had a median value of 4.0 $INP_{-10}\,cm^{-2}$ with a multiplicative standard deviation of $^{x}/1.5$ (i.e. 68 % of leaf samples at the top of

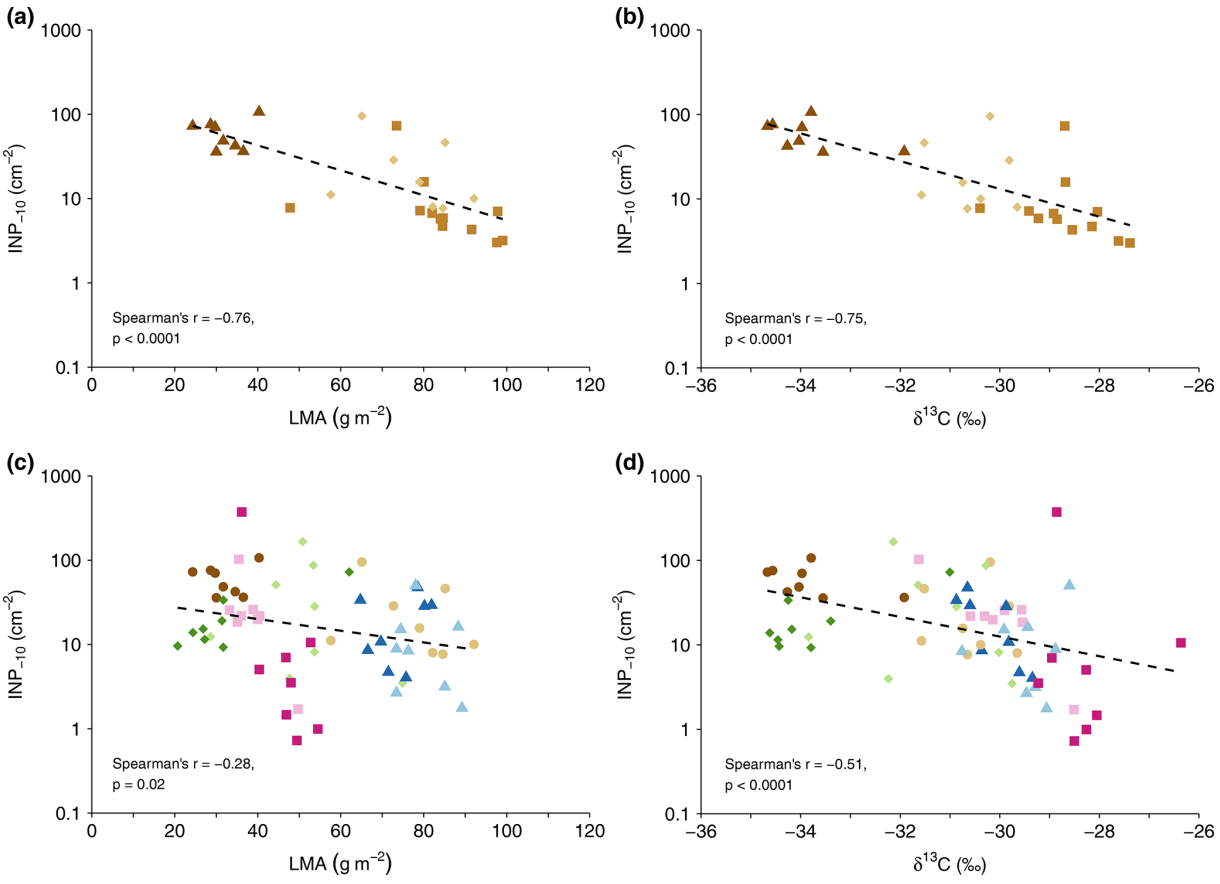

Figure 2. Cumulative INP_{-10} concentration versus leaf mass per area (LMA) **(a, c)** and leaf $\delta^{13}C$ values **(b, d)** for the GEP data set **(c, d)** and all *F. sylvatica* samples **(a, b)**. Colours and symbols represent tree species (brown circles: *F. sylvatica*, blue triangles: *P. avium*, green diamonds: *J. regia*, red squares: *T. platyphyllos*), with light colours for the first and dark colours for the second tree sampled **(c, d)**. *F. sylvatica* sampled at Hölstein is represented by squares in the top panels **(a, b)**.

the tree had a concentration between 2.7 (4.0/1.5) and 6.0 (4.0×1.5) $INP_{-10}\,cm^{-2}$). On the first sampling day, INP_{-10} concentrations were highest in the sample from the lowest position within the canopy and facing a SE direction, with concentrations 10 times (73.1 $INP_{-10}\,cm^{-2}$) higher than at the opposite side of the canopy at the same height. Five weeks later, concentrations at the lowest position facing a SE direction had decreased distinctly from 73.1 to 15.8 $INP_{-10}\,cm^{-2}$ but were still twice as high as at the opposite canopy side. These differences might be attributed to variations in the leaf microclimate or localized plant reactions. As expected from previous findings (Bachofen et al., 2020; Matyssek et al., 2010), LMA was greater at the tree top ($94.7\,g\,m^{-2} \pm 6.8\,g\,m^{-2}$) compared to the lowest part of the canopy ($70.1\,g\,m^{-2} \pm 15.2\,g\,m^{-2}$, $n = 4$). Likewise, $\delta^{13}C$ values increased with height in the canopy (bottom of $-29.3‰ \pm 0.8‰$, top of $-27.8‰ \pm 0.4‰$, $n = 4$, respectively), similar to what had been reported for temperate forests before (Garten and Taylor, 1992; Hanba et al., 1997; Schleser, 1990).

The leaf mass per area and $\delta^{13}C$ covaried in both the HOL and GEP data set. The concentration of INP_{-10} tended to be higher on leaves with lower LMA and lower $\delta^{13}C$ values (Fig. 2). Both parameters did not correlate with leaf N content. Differences in LMA within broadleaf trees result primarily from variations in light availability (Matyssek et al., 2010). In the absence of variations in the atmospheric $\delta^{13}C$, leaf $\delta^{13}C$ in C_3 plants is largely determined by the stomatal aperture and photosynthetic rate (Farquhar et al., 1982). Enhanced $\delta^{13}C$ values are observed when photosynthetic rates are high or stomates are closed, e.g. under elevated light intensity or water stress (Farquhar et al., 1982; Schleser, 1990; Waring and Silvester, 1994).

The change in INP_{-10} concentrations with LMA and $\delta^{13}C$ might be linked to morphological and physiological differences between sun and shade leaves or differences in the microhabitat and microclimate that are related to variations in LMA and $\delta^{13}C$. Our results from Hölstein indicate that INP_{-10} concentrations are lower on leaves more exposed to sunlight in a canopy. Such leaves on the upper and outer part of a canopy might be in general more exposed to stressors or

processes potentially removing INPs from leaves compared to leaves on other parts of the canopy. Additionally, gradients in parameters such as RH within forest canopies (Zahnd et al., 2023) might lead to decreasing INP_{-10} concentrations towards the canopy top.

3.2 Differential INP concentrations

3.2.1 Spectral types on foliage

Of the 64 foliage samples collected at GEP, 53 displayed two clearly discriminable patterns in differential INP spectra between −3 and −10 °C. In 28 samples, differential INP concentrations increased persistently with each 1 °C step in cooling (monotonous spectral type). The remaining 25 samples exhibited one ($n = 23$) or two ($n = 2$) significant peaks (Sect. 2.3) at temperatures ranging from −3.5 to −8.5 °C (numbers indicate the centre of 1 °C temperature intervals implemented in the assays). Most of these peaks occurred around −8.5 °C (11 peaks) and −7.5 °C (9 peaks). Significant peaks at warmer temperatures were rarer (3 peaks each at −6.5 and −4.5 °C, 1 peak at −3.5 °C). Generally, discontinuous differential INP spectra indicate that a sample contains distinct INP populations (Vali, 1971). Concurrently, the fraction of INPs among aerosol particles is higher at greater supercooling, and the number of airborne INPs was often found to increase roughly exponentially with decreasing temperatures (Fletcher, 1962; Kanji et al., 2017; Li et al., 2022). This often-described relationship is equivalent to the monotonous spectral type displaying a persistent increase in differential INP concentrations with progressing cooling.

According to their efficiency, bacterial INPs are categorized as either type I, II or III, corresponding to a decrease in nucleation temperature. Type I INPs are active above −5 °C, while type III INPs nucleate ice only below −7 °C. Type II INPs are typically less abundant and induce freezing between −5 and −7 °C (Yankofsky et al., 1981). Five of the seven spectra exhibiting peaks at temperatures of > -7.5 °C occurred in *J. regia* (Fig. 3). In contrast, such type I and II modes were never found in *F. sylvatica* and were found only once in *T. platyphyllos* and *P. avium*. Samples from *F. sylvatica* predominantly featured the monotonous spectral type. This applied to *F. sylvatica* at GEP as well as at HOL. Peaks in differential INP spectra in *P. avium* tended to be at a slightly colder temperature, and the monotonous spectral type was more abundant than in *T. platyphyllos*. These differences indicate that variations in leaf habitat properties, such as the microclimate, leaf morphology and physiology, and co-occurring differences in the phyllosphere microbiome between tree species might have contributed variation to the distribution of spectral types among species. Overall, however, the pattern of differential freezing spectra and the INP_{-10} concentration differed widely between samples even within the same species. When combined, spectra of all species sampled on a particular day did also show the two discriminable patterns in differential INP spectra (Fig. S3).

Cumulative INP_{-10} concentrations did not vary systematically between spectral types (Kruskal–Wallis test, $p > 0.05$). Significant peaks at temperatures of > -7.5 °C were observed at total concentrations as low as 4.7 $INP_{-10}\,cm^{-2}$ and significant type I peaks at total concentrations as low as 8.2 $INP_{-10}\,cm^{-2}$. This indicates that the occurrence of highly efficient INPs was not solely dependent on the total number of $INPs_{-10}$.

Studies suggest that the expression and arrangement of IN proteins is substantially influenced by environmental conditions and microhabitat characteristics, including differences between host plant species (Hirano and Upper, 1989; Lindow et al., 1982; O'Brien and Lindow, 1988; Ruggles et al., 1993; Yang et al., 2022). For example, UV and γ radiation (de Araujo et al., 2019; Govindarajan and Lindow, 1988), desiccation (de Araujo et al., 2019), decreasing pH (Lukas et al., 2022) and high temperatures around 30 °C (Nemecek-Marshall et al., 1993) seem to trigger the dissolution of IN protein complexes, whereas lower temperatures around 15 °C and nutrient limitation can promote their formation (Nemecek-Marshall et al., 1993; Ruggles et al., 1993).

The larger an IN protein cluster and the higher the resultant nucleation temperature of the proteinaceous INP, the faster its activation temperature is lowered by certain stressors, e.g. radiation (Govindarajan and Lindow, 1988). Once exposed to such a stressor, an initially efficient INP will nucleate ice only at colder temperatures (Ruggles et al., 1993). The gradual breakup of larger IN protein clusters under continued stress in unfavourable conditions or the inhibition of INP cluster formation could be one possible explanation for the development of the monotonous spectral type. This explanation would imply that conditions for the expression and aggregation of IN proteins were less suitable on leaves of *F. sylvatica* as compared to the leaves of the other investigated tree species. Another explanation could be host-specific properties of *F. sylvatica* leading to a limited set of INP-producing microorganisms that generate the monotonous spectral type only.

Overall, none of the investigated leaf traits seem to explain variations in spectral patterns between leaves or tree species. Yet, other differences in the microhabitat, for example due to variations in cuticle characteristics, leaf wettability, leaf exudates or leaf topography (Yan et al., 2022), might have contributed to the unequal distribution of spectral patterns between tree species. These factors can impact the availability of water or nutrients on leaf surfaces, thereby affecting the population size and perhaps also the composition of epiphytic (INA) microorganisms. In addition, there is a link between nutrient availability and the frequency at which ice-nucleating activity is expressed in certain INA species (Nemecek-Marshall et al., 1993; Ruggles et al., 1993). As described above, environmental parameters such as temperature and moisture affect INA microorganisms (Hirano and

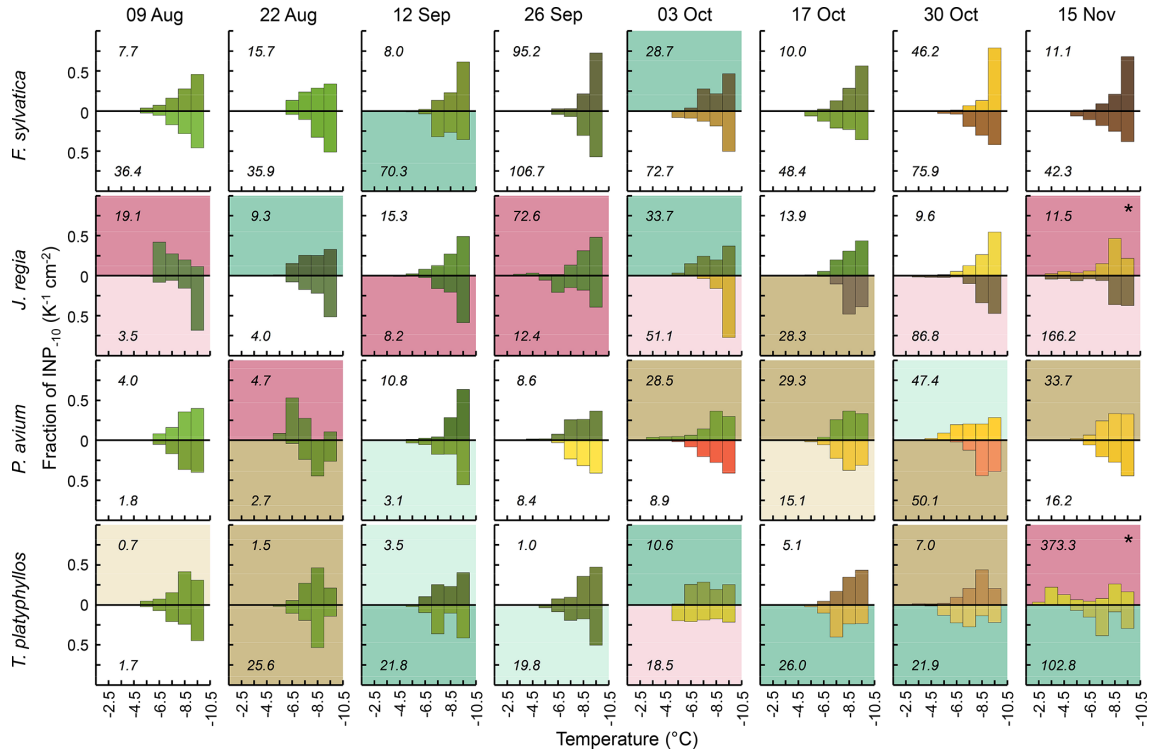

Figure 3. Differential INP concentrations (1 K temperature intervals) for tree species (rows) sampled in Gempen on all sampling days (columns), normalized to the cumulative INP_{-10} concentration (numbers in the panels). Both samples per tree species and the date are shown (above and below the x axis). Colours reflect leaf colours; panel background colour indicates the spectral type (white: monotonous spectral type, brown: peak at −8.5 °C, green: peak at −7.5 °C, purple: peak > −7.5 °C). Dark-brown, dark-green and dark-purple panel backgrounds are for spectra with significant peaks, light brown, light green and light purple panel backgrounds are for spectra with insignificant peaks (Sect. 2.3). The asterisk marks spectra with two significant peaks: one peak at > −7.5 °C and one peak at −8.5 °C.

Upper, 1989; Leben, 1988). These parameters can vary on short spatial scales within single canopies (Batzer et al., 2008; Körner and Hiltbrunner, 2018), and variations in microclimate as well as localized plant reactions might have contributed to variations in spectral patterns between leaves of the same species. In summary, the abundance of $INPs_{-10}$ and the pattern of differential freezing spectra seem to be less influenced by intrinsic leaf properties than by external conditions.

3.2.2 Comparison between foliage and air samples in terms of INPs

At GEP, we observed a median of 16 $INP_{-10}\,cm^{-2}$. This is equivalent to the median INP_{-10} concentration we observed in 3.2 m^3 of air at Jungfraujoch. Interestingly, the three most frequent spectral types among the clearly discriminable patterns at GEP – the monotonous spectral type and the spectral types with significant peaks at −8.5 and −7.5 °C – were also prevalent in similar proportions of air samples with clearly defined spectral patterns at Jungfraujoch (Fig. 4). This consistency lends support to the hypothesis that plant surfaces contribute the majority of $INPs_{-10}$ to air masses above the Alps, at least during summer and autumn. During periods with the admixture of air from the planetary boundary layer (PBL), particles emitted from local and regional sources in the airshed of JFJ can be transported to the high-altitude site. In summer, such PBL injections occur frequently and are mainly driven by thermally induced processes such as convective PBL growth, anabatic mountain winds and mountain venting (Collaud Coen et al., 2011; Griffiths et al., 2014; Henne et al., 2004; Ketterer et al., 2014; Poltera et al., 2017). Additionally, frontal systems and dynamically driven winds can lift air from the PBL above the Alps (Ketterer et al., 2014; Lothon et al., 2003).

Our findings also suggest that the same parameter or set of parameters controls the aggregation of IN proteins on the scale of leaves within a canopy as in the wider landscape (i.e. airshed upwind of JFJ). Such a driver could, for example, be the leaf wetness duration. It varies within single canopies (Batzer et al., 2008) and within a similar range (< 4 to around 10 $h\,d^{-1}$), as well as on the scale of entire landscapes (Asadi and Tian, 2021). Within a canopy, local differences in shading, radiative and convective cooling, and wind exposure drive variations in leaf wetness duration (Batzer et al., 2008). Within the landscape, meteorological parameters

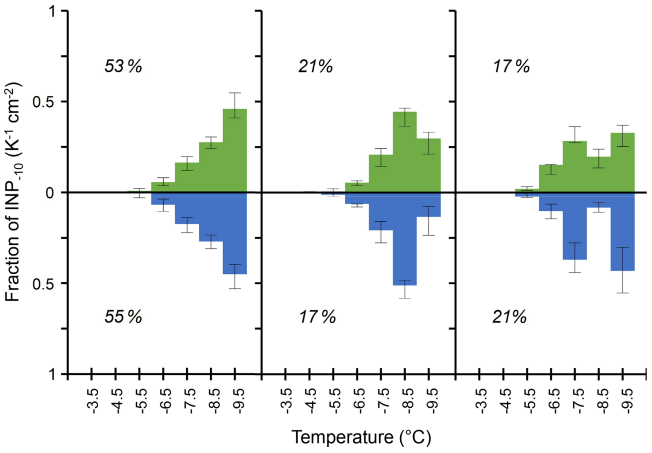

Figure 4. Median values of the three most abundant types of differential INP spectra observed on tree leaves (green) in Gempen (650 m a.s.l., $n = 53$) and in the air (blue) at Jungfraujoch (3580 m a.s.l., $n = 53$), normalized to the cumulative INP_{-10} concentration considering the spectra with a monotonous increase in differential INP concentrations with decreasing temperature and spectra with statistically significant peaks (Sect. 2.3). Indicated percentages are the relative frequency of each spectral type among spectra with clearly defined patterns found on foliage and in the air, respectively, with error bars for the 1st and 3rd quartile. Note that the number of analysed droplets per sample is different between Gempen (144) and Jungfraujoch (52).

such as RH and potential evaporation are good predictors of leaf wetness duration (Asadi and Tian, 2021; Gleason et al., 2008). The effect of RH on $INPs_{-10}$ (Fig. 1) hints at moisture affecting not only the size of epiphytic bacterial populations (Caristi et al., 1991) but also the INP density in the phyllosphere. Consequently, the varying availability of moisture could possibly provide part of the explanation for both temporal trends (Fig. 1) and differences in INP populations between samples (Fig. 2) observed in this study. An indication of the influence of environmental conditions on biological INP populations aligns with observed differences in the abundance of leaf-litter-derived INPs between climatic zones (Schnell and Vali, 1976) as well as the influence of meteorological parameters on INA bacteria colonizing crops (Hirano and Upper, 1989; Leben, 1988). The similarity in spectral types and their relative abundance between tree canopies and air at JFJ further suggests a certain consistency in freezing spectra between vegetation types covering a large share of terrestrial surface, e.g. forest, grassland and agricultural crops which also harbour INA microorganisms (Hill et al., 2014; Lindemann et al., 1982; Lindow et al., 1978a). Thus, the similarity in INP abundance and spectra among the four investigated tree species might apply to a broader range of trees and other growth forms.

4 Conclusions

To conclude, our results indicate that changes in meteorological parameters, such as RH and possibly temperature, by affecting the leaf microhabitat, impact the concentration and perhaps activity of INA microorganisms in plant canopies. The similarity in spectral types and their relative abundance between tree canopies upwind of JFJ and in the air at JFJ are a novel type of evidence for plant surfaces being a major source of biological INPs at cloud height above the Alps. If increasing RH or decreasing temperature leads to an enhanced INP supply at plant surfaces, the flux of biological INPs from the phyllosphere to the atmosphere might be elevated under these conditions, even in the absence of additional emission mechanisms. Therefore, at locations in the atmosphere where mixed-phase clouds can form and INPs originating from the phyllosphere comprise a large part of the biological INP population, changes in meteorological conditions, beyond rainfall (Mignani et al., 2021), could impact the INP source and, thereby, cloud development. Further exploration and quantification of the effect of meteorological parameters on biological INP populations on leaves might reveal interesting insights into the dynamics of the INP distribution at mixed-phase cloud height.

Data availability. Leaf data discussed herein are provided in the Supplement of this article. Data collected at Jungfraujoch are available upon request from the corresponding author.

Supplement. The supplement related to this article is available online at: https://doi.org/10.5194/bg-21-5219-2024-supplement.

Author contributions. AE and FC designed the study. AE conducted experiments at Jungfraujoch and analysed the data. AE and FC collected and analysed leaf data. AE wrote the manuscript with contributions from FC.

Competing interests. The contact author has declared that neither of the authors has any competing interests.

Disclaimer. Publisher's note: Copernicus Publications remains neutral with regard to jurisdictional claims made in the text, published maps, institutional affiliations, or any other geographical representation in this paper. While Copernicus Publications makes every effort to include appropriate place names, the final responsibility lies with the authors.

Acknowledgements. Sampling a vertical profile of a *Fagus sylvatica* individual in Hölstein was possible thanks to the Swiss Canopy Crane II, a research site financially supported by the Swiss Federal

Office for the Environment (FOEN) and the University of Basel. We thank the crane operator, Niek ten Cate, for his support during sampling in Hölstein and Linus Keiser and Jean-Luc Mosimann for their help during the analysis of leaf carbon and nitrogen content. We are grateful to the International Foundation of the High Altitude Research Stations Jungfraujoch and Gornergrat (HFSJG), 3012 Bern, Switzerland, for providing us the opportunity to work and conduct experiments at the high-altitude Jungfraujoch observatory. We thank Stephan Henne for performing FLEXPART simulations for us, which we included in the reply to the general comment of referee no. 2. We acknowledge financial support for this study from the Swiss National Science Foundation (SNSF; grant no. 200020-212121).

Financial support. This research has been supported by the Swiss National Science Foundation (SNSF, grant no. 200020-212121).

Review statement. This paper was edited by Paul Stoy and reviewed by two anonymous referees.

References

Anderson, J. A., Buchanan, D. W., Stall, R. E., and Hall, C. B.: Frost Injury of Tender Plants Increased by *Pseudomonas syringae* van Hall[1], J. Am. Soc. Hortic. Sci., 107, 123–125, https://doi.org/10.21273/JASHS.107.1.123, 1982.

Anonymous: Mitteleuropäische Waldbaumarten – Artbeschreibung und ökologie unter besonderer Berücksichtigung der Schweiz, ETH Zürich, https://ethz.ch/content/dam/ethz/special-interest/usys/ites/waldmgmt-waldbau-dam/documents/Lehrmaterialien/Skripte/Baumartenbeschreibungen/ME-Waldbaumarten (last access: 10 November 2024), 2002.

Asadi, P. and Tian, D.: Estimating leaf wetness duration with machine learning and climate reanalysis data, Agr. Forest Meteorol., 307, 108548, https://doi.org/10.1016/j.agrformet.2021.108548, 2021.

Bachofen, C., D'Odorico, P., and Buchmann, N.: Light and VPD gradients drive foliar nitrogen partitioning and photosynthesis in the canopy of European beech and silver fir, Oecologia, 192, 323–339, 2020.

Batzer, J. C., Gleason, M. L., Taylor, S. E., Koehler, K. J., and Monteiro, J. E. B. A.: Spatial Heterogeneity of Leaf Wetness Duration in Apple Trees and Its Influence on Performance of a Warning System for Sooty Blotch and Flyspeck, Plant Dis., 92, 164–170, https://doi.org/10.1094/PDIS-92-1-0164, 2008.

Beattie, G. A.: Water relations in the interaction of foliar bacterial pathogens with plants, Annu. Rev. Phytopathol., 49, 533–555, https://doi.org/10.1146/annurev-phyto-073009-114436, 2011.

Beattie, G. A. and Lindow, S. E.: The Secret Life of Foliar Bacterial Pathogens on Leaves, Annu. Rev. Phytopathol., 33, 145–172, https://doi.org/10.1146/annurev.py.33.090195.001045, 1995.

Beyeler, A., Douard, R., Jeannet, A., Willi-Tobler, L., and Weibel, F.: Land use in Switzerland – Results of the Swiss land use statistics 2018, Federal Statistical Office (FSO), Neuchâtel, Switzerland, https://www.bfs.admin.ch/asset/en/19365054 (last access: 10 November 2024), 2021.

Burrows, S. M., McCluskey, C. S., Cornwell, G., Steinke, I., Zhang, K., Zhao, B., Zawadowicz, M., Raman, A., Kulkarni, G., China, S., Zelenyuk, A., and DeMott, P. J.: Ice-Nucleating Particles That Impact Clouds and Climate: Observational and Modeling Research Needs, Rev. Geophys., 60, e2021RG000745, https://doi.org/10.1029/2021RG000745, 2022.

Caristi, J., Sands, D. C., and Georgakopoulos, D. G.: Simulation of epiphytic bacterial growth under field conditions, Simulation, 56, 295–301, https://doi.org/10.1177/003754979105600505, 1991.

Collaud Coen, M., Weingartner, E., Furger, M., Nyeki, S., Prévôt, A. S. H., Steinbacher, M., and Baltensperger, U.: Aerosol climatology and planetary boundary influence at the Jungfraujoch analyzed by synoptic weather types, Atmos. Chem. Phys., 11, 5931–5944, https://doi.org/10.5194/acp-11-5931-2011, 2011.

Conen, F., Morris, C. E., Leifeld, J., Yakutin, M. V., and Alewell, C.: Biological residues define the ice nucleation properties of soil dust, Atmos. Chem. Phys., 11, 9643–9648, https://doi.org/10.5194/acp-11-9643-2011, 2011.

Conen, F., Einbock, A., Mignani, C., and Hüglin, C.: Measurement report: Ice-nucleating particles active $\geq -15\,^{\circ}\mathrm{C}$ in free tropospheric air over western Europe, Atmos. Chem. Phys., 22, 3433–3444, https://doi.org/10.5194/acp-22-3433-2022, 2022.

Coplen, T. B.: RSIL: Report of Stable Isotopic Composition for reference material USGS40, U.S. Geological Survey, https://www.usgs.gov/media/files/rsil-report-stable-isotopic-composition-reference-material-usgs40 (last access: 10 November 2024), 2019a.

Coplen, T. B.: RSIL: Report of Stable Isotopic Composition for reference materials USGS61 USGS62 and USGS63, U.S. Geological Survey, https://www.usgs.gov/media/files/rsil-report-stable-isotopic-composition-reference-materials-usgs61-usgs62-and-usgs63 (last access: 10 November 2024), 2019b.

Cornwell, G. C., McCluskey, C. S., Hill, T. C. J., Levin, E. T., Rothfuss, N. E., Tai, S.-L., Petters, M. D., DeMott, P. J., Kreidenweis, S., Prather, K. A., and Burrows, S. M.: Bioaerosols are the dominant source of warm-temperature immersion-mode INPs and drive uncertainties in INP predictability, Sci. Adv., 9, eadg3715, https://doi.org/10.1126/sciadv.adg3715, 2023.

de Araujo, G. G., Rodrigues, F., Gonçalves, F. L. T., and Galante, D.: Survival and ice nucleation activity of *Pseudomonas syringae* strains exposed to simulated high-altitude atmospheric conditions, Sci. Rep.-UK, 9, 7768, https://doi.org/10.1038/s41598-019-44283-3, 2019.

Doan, H. K., Ngassam, V. N., Gilmore, S. F., Tecon, R., Parikh, A. N., and Leveau, J. H. J.: Topography-Driven Shape, Spread, and Retention of Leaf Surface Water Impacts Microbial Dispersion and Activity in the Phyllosphere, Phytobiomes J., 4, 268–280, https://doi.org/10.1094/PBIOMES-01-20-0006-R, 2020.

Einbock, A.: Quantifying the flux of ice nucleating particles from lowlands to an altitude where primary ice can be formed in clouds, MSc Thesis, University of Basel, Basel, 69 pp., 2023.

Einbock, A. and Conen, F.: Frost-free zone on leaves revisited, P. Natl. Acad. Sci. USA, 121, e2407062121, https://doi.org/10.1073/pnas.2407062121, 2024.

Farquhar, G., O'Leary, M. H. O., and Berry, J.: On the relationship between carbon isotope discrimination and the intercellular carbon dioxide concentration in leaves, Aust. J. Plant Physiol., 9, 121–137, 1982.

Felgitsch, L., Baloh, P., Burkart, J., Mayr, M., Momken, M. E., Seifried, T. M., Winkler, P., Schmale III, D. G., and Grothe, H.: Birch leaves and branches as a source of ice-nucleating macromolecules, Atmos. Chem. Phys., 18, 16063–16079, https://doi.org/10.5194/acp-18-16063-2018, 2018.

Fletcher, N. H.: The physics of rainclouds, Cambridge University Press, Cambridge, UK, 410 pp., ISBN 9780521154796, 1962.

Garten, C. T. and Taylor, G. E.: Foliar δ^{13}C within a temperate deciduous forest: spatial, temporal, and species sources of variation, Oecologia, 90, 1–7, https://doi.org/10.1007/BF00317801, 1992.

Gleason, M. L., Duttweiler, K. B., Batzer, J. C., Taylor, S. E., Sentelhas, P. C., Monteiro, J. E. B. A., and Gillespie, T. J.: Obtaining weather data for input to crop disease-warning systems: leaf wetness duration as a case study, Sci. Agr., 65, 76–87, https://doi.org/10.1590/S0103-90162008000700013, 2008.

Govindarajan, A. G. and Lindow, S. E.: Size of bacterial ice-nucleation sites measured in situ by radiation inactivation analysis, P. Natl. Acad. Sci. USA, 85, 1334–1338, https://doi.org/10.1073/pnas.85.5.1334, 1988.

Griffiths, A. D., Conen, F., Weingartner, E., Zimmermann, L., Chambers, S. D., Williams, A. G., and Steinbacher, M.: Surface-to-mountaintop transport characterised by radon observations at the Jungfraujoch, Atmos. Chem. Phys., 14, 12763–12779, https://doi.org/10.5194/acp-14-12763-2014, 2014.

Grinberg, M., Orevi, T., Steinberg, S., and Kashtan, N.: Bacterial survival in microscopic surface wetness, eLife, 8, e48508, https://doi.org/10.7554/eLife.48508, 2019.

Grose, M.: Reading the colours of plants at a finer scale, J. Landsc. Archit., 9, 42–47, https://doi.org/10.1080/18626033.2014.898829, 2014.

Grose, M.: Green leaf colours in a suburban Australian hotspot: Colour differences exist between exotic trees from far afield compared with local species, Landscape Urban Plan., 146, 20–28, https://doi.org/10.1016/j.landurbplan.2015.10.003, 2016.

Gute, E. and Abbatt, J. P. D.: Ice nucleating behavior of different tree pollen in the immersion mode, Atmos. Environ., 231, 117488, https://doi.org/10.1016/j.atmosenv.2020.117488, 2020.

Haga, D. I., Burrows, S. M., Iannone, R., Wheeler, M. J., Mason, R. H., Chen, J., Polishchuk, E. A., Pöschl, U., and Bertram, A. K.: Ice nucleation by fungal spores from the classes *Agaricomycetes*, *Ustilaginomycetes*, and *Eurotiomycetes*, and the effect on the atmospheric transport of these spores, Atmos. Chem. Phys., 14, 8611–8630, https://doi.org/10.5194/acp-14-8611-2014, 2014.

Hanba, Y. T., Mori, S., Lei, T. T., Koike, T., and Wada, E.: Variations in leaf δ^{13}C along a vertical profile of irradiance in a temperate Japanese forest, Oecologia, 110, 253–261, https://doi.org/10.1007/s004420050158, 1997.

Hård, A. and Sivik, L.: NCS–Natural Color System: A Swedish Standard for Color Notation, Color Res. Appl., 6, 129–138, https://doi.org/10.1002/col.5080060303, 1981.

Hawker, R. E., Miltenberger, A. K., Wilkinson, J. M., Hill, A. A., Shipway, B. J., Cui, Z., Cotton, R. J., Carslaw, K. S., Field, P. R., and Murray, B. J.: The temperature dependence of ice-nucleating particle concentrations affects the radiative properties of tropical convective cloud systems, Atmos. Chem. Phys., 21, 5439–5461, https://doi.org/10.5194/acp-21-5439-2021, 2021.

Henne, S., Furger, M., Nyeki, S., Steinbacher, M., Neininger, B., de Wekker, S. F. J., Dommen, J., Spichtinger, N., Stohl, A., and Prévôt, A. S. H.: Quantification of topographic venting of boundary layer air to the free troposphere, Atmos. Chem. Phys., 4, 497–509, https://doi.org/10.5194/acp-4-497-2004, 2004.

Hill, T. C. J., Moffett, B. F., DeMott, P. J., Georgakopoulos, D. G., Stump, W. L., and Franc, G. D.: Measurement of Ice Nucleation-Active Bacteria on Plants and in Precipitation by Quantitative PCR, Appl. Environ. Microb., 80, 1256–1267, https://doi.org/10.1128/AEM.02967-13, 2014.

Hill, T. C. J., DeMott, P. J., Tobo, Y., Fröhlich-Nowoisky, J., Moffett, B. F., Franc, G. D., and Kreidenweis, S. M.: Sources of organic ice nucleating particles in soils, Atmos. Chem. Phys., 16, 7195–7211, https://doi.org/10.5194/acp-16-7195-2016, 2016.

Hirano, S. S. and Upper, C. D.: Diel Variation in Population Size and Ice Nucleation Activity of *Pseudomonas syringae* on Snap Bean Leaflets, Appl. Environ. Microb., 55, 623–630, https://doi.org/10.1128/aem.55.3.623-630.1989, 1989.

Hirano, S. S., Baker, L. S., and Upper, C. D.: Raindrop Momentum Triggers Growth of Leaf-Associated Populations of *Pseudomonas syringae* on Field-Grown Snap Bean Plants, Appl. Environ. Microb., 62, 2560–2566, 1996.

Hiranuma, N., Möhler, O., Yamashita, K., Tajiri, T., Saito, A., Kiselev, A., Hoffmann, N., Hoose, C., Jantsch, E., Koop, T., and Murakami, M.: Ice nucleation by cellulose and its potential contribution to ice formation in clouds, Nat. Geosci., 8, 273–277, https://doi.org/10.1038/ngeo2374, 2015.

Huang, S., Hu, W., Chen, J., Wu, Z., Zhang, D., and Fu, P.: Overview of biological ice nucleating particles in the atmosphere, Environ. Int., 146, 106197, https://doi.org/10.1016/j.envint.2020.106197, 2021.

Jordan, D. N. and Smith, W. K.: Energy balance analysis of nighttime temperatures and forest formation in a subalpine environment, Agric. Forest Meteorol., 71, 359–372, 1994.

Kahmen, A., Basler, D., Hoch, G., Link, R. M., Schuldt, B., Zahnd, C., and Arend, M.: Root water uptake depth determines the hydraulic vulnerability of temperate European tree species during the extreme 2018 drought, Plant. Biol., 24, 1224–1239, https://doi.org/10.1111/plb.13476, 2022.

Kanji, Z. A., Ladino, L. A., Wex, H., Boose, Y., Burkert-Kohn, M., Cziczo, D. J., and Krämer, M.: Overview of Ice Nucleating Particles, Meteorol. Monogr., 58, 1.1–1.33, https://doi.org/10.1175/AMSMONOGRAPHS-D-16-0006.1, 2017.

Ketterer, C., Zieger, P., Bukowiecki, N., Collaud Coen, M., Maier, O., Ruffieux, D., and Weingartner, E.: Investigation of the Planetary Boundary Layer in the Swiss Alps Using Remote Sensing and In Situ Measurements, Bound.-Lay. Meteorol., 151, 317–334, https://doi.org/10.1007/s10546-013-9897-8, 2014.

Kim, H. K., Orser, C., Lindow, S. E., and Sands, D. C.: *Xanthomonas campestris* pv. translucens Strains Active in Ice Nucleation, Plant Dis., 71, 994–997, 1987.

Kinkel, L. L.: Microbial Population Dynamics on Leaves, Annu. Rev. Phytopathol., 35, 327–347, https://doi.org/10.1146/annurev.phyto.35.1.327, 1997.

Kinney, N. L. H., Hepburn, C. A., Gibson, M. I., Ballesteros, D., and Whale, T. F.: High interspecific variability in ice nucleation activity suggests pollen ice nucleators are incidental, Biogeosciences, 21, 3201–3214, https://doi.org/10.5194/bg-21-3201-2024, 2024.

Körner, C. and Hiltbrunner, E.: The 90 ways to describe plant temperature, Perspect. Plant Ecol. Evol., 30, 16–21, https://doi.org/10.1016/j.ppees.2017.04.004, 2018.

Latham, J. S., Cumani, R., Rosati, I., and Bloise, M.: FAO Global Land Cover (GLC-SHARE) database Beta-Release Version 1.0 Database, Land and Water Division, https://www.fao.org/uploads/media/glc-share-doc.pdf (last access: 10 November 2024), 2014.

Leben, C.: Relative humidity and the survival of epiphytic bacteria with buds and leaves of cucumber plants, Phytopathology, 78, 179–185, 1988.

Li, G., Wieder, J., Pasquier, J. T., Henneberger, J., and Kanji, Z. A.: Predicting atmospheric background number concentration of ice-nucleating particles in the Arctic, Atmos. Chem. Phys., 22, 14441–14454, https://doi.org/10.5194/acp-22-14441-2022, 2022.

Lim, P. O., Kim, H. J., and Nam, H. G.: Leaf senescence, Annu. Rev. Plant Biol., 58, 115–136, https://doi.org/10.1146/annurev.arplant.57.032905.105316, 2007.

Limpert, E., Stahel, W. A., and Abbt, M.: Log-normal Distributions across the Sciences: Keys and Clues, BioScience, 51, 341–352, https://doi.org/10.1641/0006-3568(2001)051[0341:LNDATS]2.0.CO;2, 2001.

Lindemann, J., Constantinidou, H. A., Barchet, W. R., and Upper, C. D.: Plants as Sources of Airborne Bacteria, Including Ice Nucleation-Active Bacteria, Appl. Environ. Microb., 44, 1059–1063, 1982.

Lindow, S. E., Arny, D. C., and Upper, C. D.: Distribution of ice nucleation-active bacteria on plants in nature, Appl. Environ. Microb., 36, 831–838, 1978a.

Lindow, S. E., Arny, D. C., and Upper, C. D.: Erwinia herbicola: A Bacterial Ice Nucleus Active in Increasing Frost Injury to Corn, Phytopathology, 68, 523–527, https://doi.org/10.1094/Phyto-68-523, 1978b.

Lindow, S. E., Hirano, S. S., Barchet, W. R., Arny, D. C., and Upper, C. D.: Relationship between Ice Nucleation Frequency of Bacteria and Frost Injury, Plant. Physiol., 70, 1090–1093, https://doi.org/10.1104/pp.70.4.1090, 1982.

Lothon, M., Druilhet, A., Bénech, B., Campistron, B., Bernard, S., and Saïd, F.: Experimental study of five föhn events during the Mesoscale Alpine Programme: From synoptic scale to turbulence, Q. J. Roy. Meteorol. Soc., 129, 2171–2193, https://doi.org/10.1256/qj.02.30, 2003.

Lukas, M., Schwidetzky, R., Eufemio, R. J., Bonn, M., and Meister, K.: Toward Understanding Bacterial Ice Nucleation, J. Phys. Chem. B, 126, 1861–1867, https://doi.org/10.1021/acs.jpcb.1c09342, 2022.

Maki, L. R., Galyan, E. L., Chang-Chien, M.-M., and Caldwell, D. R.: Ice Nucleation Induced by *Pseudomonas syringae*[1], Appl. Microbiol., 28, 456–459, 1974.

Matyssek, R., Fromm, J., Rennenberg, H., and Roloff, A.: Biologie der Bäume von der Zelle zur globalen Ebene, 1st edn., Ulmer, Stuttgart, 349 pp., ISBN 9783825284503, 2010.

Mignani, C., Wieder, J., Sprenger, M. A., Kanji, Z. A., Henneberger, J., Alewell, C., and Conen, F.: Towards parameterising atmospheric concentrations of ice-nucleating particles active at moderate supercooling, Atmos. Chem. Phys., 21, 657–664, https://doi.org/10.5194/acp-21-657-2021, 2021.

Morris, C. E., Sands, D. C., Glaux, C., Samsatly, J., Asaad, S., Moukahel, A. R., Gonçalves, F. L. T., and Bigg, E. K.: Urediospores of rust fungi are ice nucleation active at $> -10\,^{\circ}\mathrm{C}$ and harbor ice nucleation active bacteria, Atmos. Chem. Phys., 13, 4223–4233, https://doi.org/10.5194/acp-13-4223-2013, 2013.

Murray, B. J., O'Sullivan, D., Atkinson, J. D., and Webb, M. E.: Ice nucleation by particles immersed in supercooled cloud droplets, Chem. Soc. Rev., 41, 6519–6554, https://doi.org/10.1039/C2CS35200A, 2012.

Nemecek-Marshall, M., LaDuca, R., and Fall, R.: High-level expression of ice nuclei in a *Pseudomonas syringae* strain is induced by nutrient limitation and low temperature, J. Bacteriol., 175, 4062–4070, https://doi.org/10.1128/jb.175.13.4062-4070.1993, 1993.

O'Brien, R. D. and Lindow, S. E.: Effect of Plant Species and Environmental Conditions on Ice Nucleation Activity of *Pseudomonas syringae* on Leaves, Appl. Environ. Microb., 54, 2281–2286, https://doi.org/10.1128/aem.54.9.2281-2286.1988, 1988.

O'Sullivan, D., Murray, B. J., Malkin, T. L., Whale, T. F., Umo, N. S., Atkinson, J. D., Price, H. C., Baustian, K. J., Browse, J., and Webb, M. E.: Ice nucleation by fertile soil dusts: relative importance of mineral and biogenic components, Atmos. Chem. Phys., 14, 1853–1867, https://doi.org/10.5194/acp-14-1853-2014, 2014.

Poltera, Y., Martucci, G., Collaud Coen, M., Hervo, M., Emmenegger, L., Henne, S., Brunner, D., and Haefele, A.: PathfinderTURB: an automatic boundary layer algorithm. Development, validation and application to study the impact on in situ measurements at the Jungfraujoch, Atmos. Chem. Phys., 17, 10051–10070, https://doi.org/10.5194/acp-17-10051-2017, 2017.

Pouleur, S., Richard, C., Martin, J. G., and Antoun, H.: Ice Nucleation Activity in *Fusarium acuminatum* and *Fusarium avenaceum*, Appl. Environ. Microb., 58, 2960–2964, https://doi.org/10.1128/aem.58.9.2960-2964.1992, 1992.

Pummer, B. G., Bauer, H., Bernardi, J., Bleicher, S., and Grothe, H.: Suspendable macromolecules are responsible for ice nucleation activity of birch and conifer pollen, Atmos. Chem. Phys., 12, 2541–2550, https://doi.org/10.5194/acp-12-2541-2012, 2012.

Qiu, Y., Hudait, A., and Molinero, V.: How Size and Aggregation of Ice-Binding Proteins Control Their Ice Nucleation Efficiency, J. Am. Chem. Soc., 141, 7439–7452, https://doi.org/10.1021/jacs.9b01854, 2019.

Richard, C., Martin, J.-G., and Pouleur, S.: Ice nucleation activity identified in some phytopathogenic *Fusarium* species, Phytoprotection, 77, 83–92, https://doi.org/10.7202/706104ar, 1996.

Ruggles, J. A., Nemecek-Marshall, M., and Fall, R.: Kinetics of appearance and disappearance of classes of bacterial ice nuclei support an aggregation model for ice nucleus assembly., J. Bacteriol., 175, 7216–7221, 1993.

Schleser, G. H.: Investigations of the δ^{13}C Pattern in Leaves of *Fagus sylvatica* L., J. Exp. Bot., 41, 565–572, 1990.

Schnell, R. C. and Vali, G.: Biogenic Ice Nuclei: Part I. Terrestrial and Marine Sources, J. Atmos. Sci., 33, 1554–1564, https://doi.org/10.1175/1520-0469(1976)033<1554:BINPIT>2.0.CO;2, 1976.

Schwidetzky, R., de Almeida Ribeiro, I., Bothen, N., Backes, A. T., DeVries, A. L., Bonn, M., Fröhlich-Nowoisky, J., Molinero, V., and Meister, K.: Functional aggregation of cell-free proteins

enables fungal ice nucleation, P. Natl. Acad. Sci. USA, 120, e2303243120, https://doi.org/10.1073/pnas.2303243120, 2023.

Seifried, T. M., Bieber, P., Felgitsch, L., Vlasich, J., Reyzek, F., Schmale III, D. G., and Grothe, H.: Surfaces of silver birch (*Betula pendula*) are sources of biological ice nuclei: in vivo and in situ investigations, Biogeosciences, 17, 5655–5667, https://doi.org/10.5194/bg-17-5655-2020, 2020.

Shen, S., Yao, Y., and Li, C.: Quantitative study on landscape colors of plant communities in urban parks based on natural color system and M-S theory in Nanjing, China, Color Res. Appl., 47, 152–163, https://doi.org/10.1002/col.22713, 2022.

Šigutová, H., Šigut, M., Pyszko, P., Kostovčík, M., Kolařík, M., and Drozd, P.: Seasonal Shifts in Bacterial and Fungal Microbiomes of Leaves and Associated Leaf-Mining Larvae Reveal Persistence of Core Taxa Regardless of Diet, Microbiol. Spectr., 11, e03160-22, https://doi.org/10.1128/spectrum.03160-22, 2023.

Stone, B. W. G. and Jackson, C. R.: Seasonal Patterns Contribute More Towards Phyllosphere Bacterial Community Structure than Short-Term Perturbations, Microb. Ecol., 81, 146–156, https://doi.org/10.1007/s00248-020-01564-z, 2021.

Stopelli, E., Conen, F., Zimmermann, L., Alewell, C., and Morris, C. E.: Freezing nucleation apparatus puts new slant on study of biological ice nucleators in precipitation, Atmos. Meas. Tech., 7, 129–134, https://doi.org/10.5194/amt-7-129-2014, 2014.

Testa, B., Hill, T. C. J., Marsden, N. A., Barry, K. R., Hume, C. C., Bian, Q., Uetake, J., Hare, H., Perkins, R. J., Möhler, O., Kreidenweis, S. M., and DeMott, P. J.: Ice Nucleating Particle Connections to Regional Argentinian Land Surface Emissions and Weather During the Cloud, Aerosol, and Complex Terrain Interactions Experiment, J. Geophys. Res.-Atmos., 126, e2021JD035186, https://doi.org/10.1029/2021JD035186, 2021.

Vali, G.: Quantitative Evaluation of Experimental Results on the Heterogeneous Freezing Nucleation of Supercooled Liquids, J. Atmos. Sci., 28, 402–409, https://doi.org/10.1175/1520-0469(1971)028<0402:QEOERA>2.0.CO;2, 1971.

Vali, G.: Revisiting the differential freezing nucleus spectra derived from drop-freezing experiments: methods of calculation, applications, and confidence limits, Atmos. Meas. Tech., 12, 1219–1231, https://doi.org/10.5194/amt-12-1219-2019, 2019.

Vorholt, J. A.: Microbial life in the phyllosphere, Nat. Rev. Microbiol., 10, 828–840, https://doi.org/10.1038/nrmicro2910, 2012.

Waring, R. H. and Silvester, W. B.: Variation in foliar δ^{13}C values within the crowns of *Pinus radiata* trees, Tree Physiol., 14, 1203–1213, https://doi.org/10.1093/treephys/14.11.1203, 1994.

Wieland, F., Bothen, N., Schwidetzky, R., Seifried, T. M., Bieber, P., Pöschl, U., Meister, K., Bonn, M., Fröhlich-Nowoisky, J., and Grothe, H.: Aggregation of ice-nucleating macromolecules from *Betula pendula* pollen determines ice nucleation efficiency, EGUsphere [preprint], https://doi.org/10.5194/egusphere-2024-752, 2024.

Wright, T. P., Hader, J. D., McMeeking, G. R., and Petters, M. D.: High Relative Humidity as a Trigger for Widespread Release of Ice Nuclei, Aerosol Sci. Technol., 48, i–v, https://doi.org/10.1080/02786826.2014.968244, 2014.

Xing, X., Hao, P., and Dong, L.: Color characteristics of Beijing's regional woody vegetation based on Natural Color System, Color Res. Appl., 44, 595–612, https://doi.org/10.1002/col.22375, 2019.

Yan, K., Han, W., Zhu, Q., Li, C., Dong, Z., and Wang, Y.: Leaf surface microtopography shaping the bacterial community in the phyllosphere: evidence from 11 tree species, Microbiol. Res., 254, 126897, https://doi.org/10.1016/j.micres.2021.126897, 2022.

Yang, S., Rojas, M., Coleman, J. J., and Vinatzer, B. A.: Identification of Candidate Ice Nucleation Activity (INA) Genes in *Fusarium avenaceum* by Combining Phenotypic Characterization with Comparative Genomics and Transcriptomics, J. Fungi, 8, 958, https://doi.org/10.3390/jof8090958, 2022.

Yankofsky, S. A., Levin, Z., Bertold, T., and Sandlerman, N.: Some Basic Characteristics of Bacterial Freezing Nuclei, J. Appl. Meteorol. Clim., 20, 1013–1019, https://doi.org/10.1175/1520-0450(1981)020<1013:SBCOBF>2.0.CO;2, 1981.

Zahnd, C., Arend, M., Kahmen, A., and Hoch, G.: Microclimatic gradients cause phenological variations within temperate tree canopies in autumn but not in spring, Agr. Forest Meteorol., 331, 109340, https://doi.org/10.1016/j.agrformet.2023.109340, 2023.